Magnetic phase of the perovskite $CaCrO_3$ studied with μ^+SR

Oren Ofer,[1,*] Jun Sugiyama,[2] Martin Månsson,[3] Kim H. Chow,[4] Eduardo J. Ansaldo,[1] Jess H. Brewer,[1,5] Masahiko Isobe,[6] and Yutaka Ueda[6]

[1]*TRIUMF, 4004 Wesbrook Mall, Vancouver, British Columbia, Canada V6T 2A3*

[2]*Toyota Central Research and Development Labs., Inc., Nagakute, Aichi 480-1192, Japan*

[3]*Laboratory for Neutron Scattering, Paul Scherrer Institute, ETH Zürich, CH-5232 Villigen PSI, Switzerland*

[4]*Department of Physics, University of Alberta, Edmonton, Alberta, Canada T6G 2G7*

[5]*CIFAR and Department of Physics and Astronomy, University of British Columbia, Vancouver, British Columbia, Canada V6T 1Z1*

[6]*Materials Design and Characterization Laboratory, Institute for Solid State Physics, University of Tokyo, Kashiwa, Chiba 277-8581, Japan*

(Received 18 January 2010; revised manuscript received 13 April 2010; published 4 May 2010)

We investigated the magnetic phase of the perovskite $CaCrO_3$ by using the muon-spin relaxation technique accompanied by susceptibility measurements. A thermal hysteresis loop is identified with a width of about 1 K at the transition temperature. Within the time scale of the muon lifetime, a static antiferromagnetic order is revealed with distinct multiple internal fields which are experienced in the muon interstitial sites below the phase-transition temperature, T_N=90 K. Above T_N, lattice deformations are indicated by transverse-field muon-spin rotation and relaxation suggesting a magnetoelastic mechanism.

DOI: 10.1103/PhysRevB.81.184405 PACS number(s): 76.75.+i, 75.50.Ee, 75.50.Lk, 74.62.Fj

I. INTRODUCTION

The coexistence of metallic conductivity *and* antiferromagnetism is uncommon and has therefore inspired theoretical[1] and experimental[2,3] interests, particularly for transition-metal oxides (MO_x), due to a strong hybridization of *d* orbital of the metal ion (*M*) and 2*p* orbital of the oxygen (O). The magnetic properties in these systems are governed mainly by a superexchange interaction via an oxygen between the nearest-neighboring (NN) *M* ions, and additionally by a competition between the NN interaction and the next-nearest-neighbor interaction. This competition has been reported to cause the magnetic order and affect the structural and electronic properties. In most experimental systems,[4,5] these interactions are characterized by low dimensionality thereby granting the exotic coexistence of the antiferromagnetic (AFM) order and metallic conductivity. The three-dimensional perovskite $CaCrO_3$ represent an exception.

Although $CaCrO_3$ was reported to show semiconducting[6] or insulating[2] properties with AFM order below 90 K ($=T_N$), recent measurements on single crystals, grown in high-pressure synthesis, indicated metallic conductivity for $CaCrO_3$ even below T_N.[7] This was also supported by infrared reflectivity measurements on a polycrystalline sample.[3] Furthermore, based on powder neutron-diffraction analysis, the AFM spin structure was proposed as a *C*-type AFM in which Cr spins order antiferromagnetically in the *ab* plane but ferromagnetically along the *c* axis.[3] A high-temperature Curie-Weiss fit of the susceptibility-versus-*T* curve in the *T* range between 400 and 600 K indicated the effective magnetic moment (μ_{eff}) of Cr to be $3.6\mu_B$ and the Weiss *T* (Θ_p) is about 920 K.[7,8] Since the Cr ions are in a 4+ state with $S=1$, the obtained μ_{eff} is rather high compared with the localized-spin-only value ($2.85\mu_B$). Moreover, it was found that the $CaCrO_3$ system has a magnetoelastic distortion driven by the Cr moments,[3] resulting in a small change in the orthorhombic lattice parameters at T_N. Despite the several macroscopic measurements mentioned above, the microscopic magnetic nature of $CaCrO_3$ has not been investigated so far because of the difficulty of sample preparation and eventually the absence of NMR-active elements in $CaCrO_3$, as the natural abundance for the NMR-active ^{43}Ca is 0.14% and that for ^{53}Cr is 9.5%.

In contrast to NMR, the muon-spin rotation and relaxation (μ^+SR) technique is applicable to all magnetic materials,[9,10] even if they lack elements with nuclear magnetic moments. We have, therefore, carried out an experimental study on the perovskite $CaCrO_3$ (see Fig. 1) by means of μ^+SR due to its remarkable ability in detecting local magnetic order, whether it is short or long ranged. Combining bulk dc susceptibility and μ^+SR measurements, we characterize the magnetic prop-

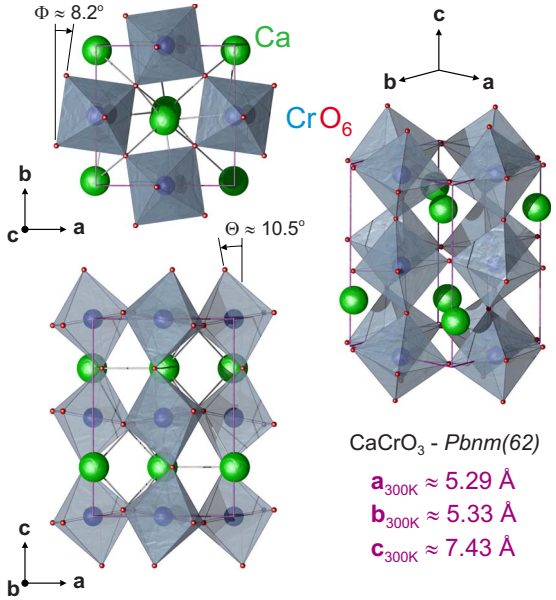

FIG. 1. (Color online) The $GdFeO_3$-type crystal structure (space group *Pbnm*, No. 62) of $CaCrO_3$ that evolves from the ideal perovskite structure by a rotation ($\Phi \approx 8.2°$) and tilt ($\Theta \approx 10.5°$) of the CrO_6 octahedra (Ref. 3). Thin purple (light gray) lines enclose the unit cell.

erties of $CaCrO_3$. Our major finding is a C_y-type AFM phase, determined from the multiple frequencies revealed in zero-field (ZF) μ^+SR. Such frequencies are the attributes of the several μ^+ interstitial sites in the AFM phase. Second, the transverse-field (TF) μ^+SR signals also suggest a deformation of the lattice, thereby corroborating that $CaCrO_3$ experiences a magnetoelastic distortion.

II. EXPERIMENT

Polycrystalline $CaCrO_3$ was prepared by a solid-state reaction of CaO and CrO_2 under 4 GPa at 1000 °C for 30 min in the Institute of Solid State Physics of University of Tokyo. dc-χ measurement (shown later) and powder diffraction were performed and agreed with previously published data. In the μ^+SR experiment, the powder sample was placed in a small envelope made of very thin Al-coated Mylar tape and attached to a low-background sample holder. In order to make certain that the muon stopped primarily inside the sample, we ensured that the side facing the muon beamline was only covered by a single layer of the mylar tape. Subsequently, ZF, TF, and longitudinal-field (LF) μ^+SR spectra were collected for $1.8 \leq T \leq 150$ K, at the M20 and M15 surface muon channel at TRIUMF, Vancouver, Canada. The experimental setup and techniques are described in detail elsewhere.[11]

III. RESULTS

The bulk magnetization and susceptibility of $CaCrO_3$ is shown in Fig. 2 as a function of T and H. The temperature dependence of the bulk dc susceptibility, χ, was measured using a commercial superconducting quantum interference device magnetometer (Magnetic Property Measurement System—Quantum Design). The magnetic transition is seen clearly at $T_N \sim 90$ K, however the $\chi(T)$ curve shows the appearance of small spontaneous magnetization below T_N, that is not of a typical AFM transition. The same $\chi(T)$ behavior is seen at all fields measured ($1 \leq H \leq 50$ kOe, not shown), therefore this can be ruled out as field induced. Figure 2(a) displays the characteristic $\chi(T)$ curves obtained on cooling and heating with an applied field of 50 kOe. In Fig. 2(c), we plot the magnetization, M, versus the field, H, taken at several temperatures, the magnetic hysteresis loop seen below T_N, at 80 and 5 K, indicates the presence of a weak ferromagnetic contribution, which is attributed from the canted spins along the c direction. To corroborate this magnetic transition, we performed weak transverse-field measurements.

A weak transverse-field (wTF) measurements, where the field applied is perpendicular to the muon-spin direction and is weak compared to any spontaneous internal fields in the ordered phase, is a sensitive probe to local magnetic order. In Fig. 2(b), we plot the T dependence of the normalized wTF asymmetry (NA_{TF}) taken at 30 Oe on heating. Note that the NA_{TF} is proportional to the volume fraction of the paramagnetic phase. The magnetic phase transition, as indicated by the wTF measurements, also identifies the transition at $T_N = 90$ K. To further explore the magnetic phase, we performed ZF μ^+SR, which is a site-sensitive probe in which the muon asymmetry is only affected by the internal magnetic fields.

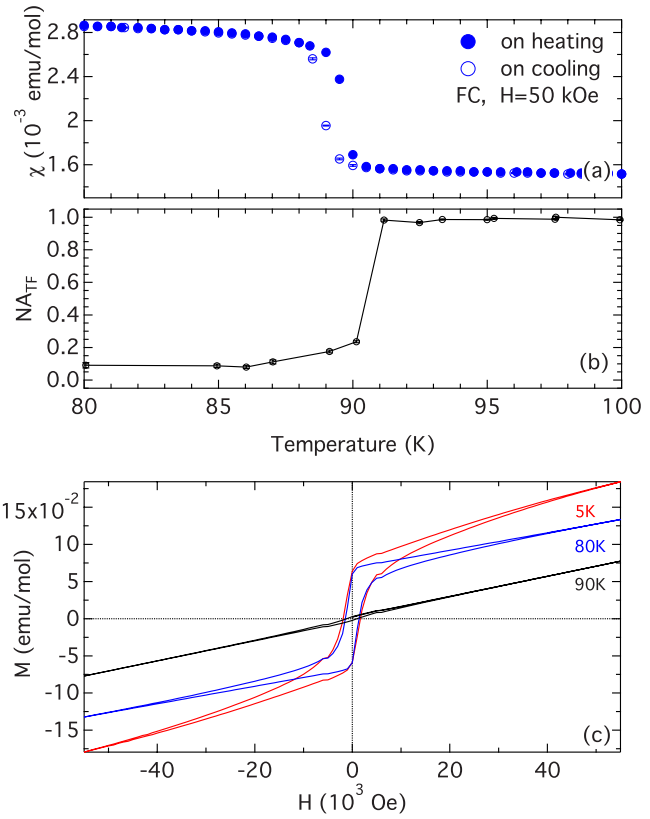

FIG. 2. (Color online) (a) The $\chi(T)$ curve at the vicinity of magnetic transition measured on cooling and on heating with $H = 50$ kOe in field cooled (FC) mode. (b) The normalized wTF Asymmetry with applied field $H = 30$ Oe. (c) The magnetization (M) versus H at 90 (black line), 80 (blue), and 5 K (red).

ZF μ^+SR measurements were taken in the same configuration as described in Sec. II. The inset of Fig. 3(a) shows the raw data taken at $T = 40$ K where the main figure displays the Fourier transform of the raw ZF spectrum. At all temperatures below T_N, the ZF spectrum exhibits multiple frequencies, which consists of mainly four frequencies. Therefore, the spectra were fitted with a sum of four oscillating signals where the asymmetry is divided into a 2/3 oscillatory and 1/3 "tail" exponentially relaxing components, namely,

$$A_0 P_{ZF}(t) = \sum_{i=1}^{4} A_{osc,i} \cos(\omega_i t) \exp(-\lambda_{osc,i} t) + A_{tail,i} \exp(-\lambda_{tail,i} t),$$

where $A_{osc} = 2A_0/3$ and $A_{tail} = A_0/3$ are the asymmetries, $\lambda_{osc} = 1/T_2$ and $\lambda_{tail} = 1/T_1$ are the relaxation rates, and ω_i are the muon Larmor frequencies of the four signals. The quality of the fit is demonstrated in the inset of Fig. 3(a) by the solid line.

Figure 3(b) summarizes the T dependence of the muon precession frequencies $[f_i = \omega_i/(2\pi)]$. The low frequencies, $i = 1, 2, 3$, are nearly independent of temperature up to 90 K

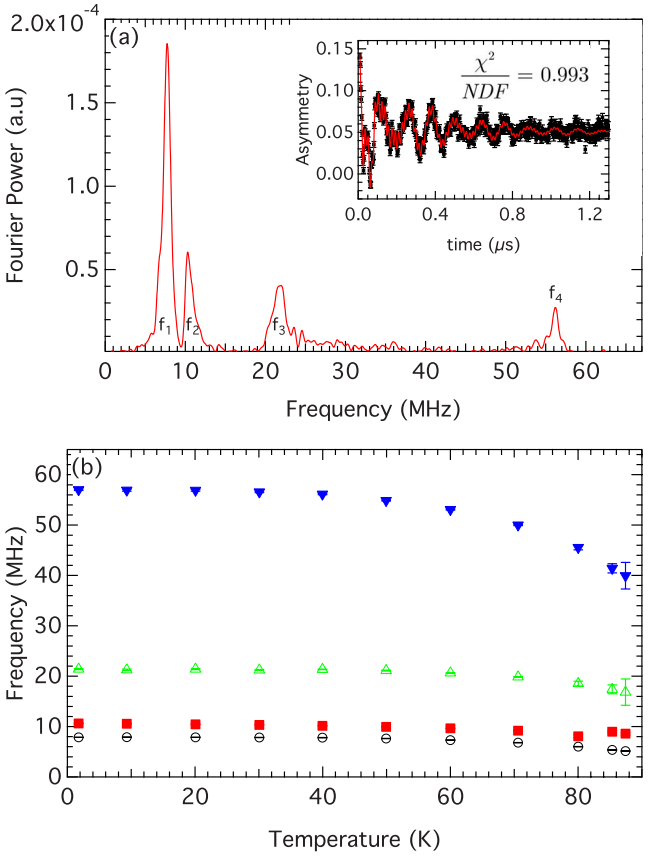

FIG. 3. (Color online) (a) The Fourier transform of the zero-field spectra at $T=40$ K. Inset shows the raw ZF asymmetry spectrum. (b) The temperature dependence of the muon precession frequencies at the AFM phase.

whereas f_4 decreases smoothly above 30 K. The amplitude (not shown) of f_4 also decreases dramatically above 50 K. We, therefore, suggest that $CaCrO_3$ displays a single AFM phase. Electrostatic potential calculations confirm that there are four possible different muon sites near O^{-2} ions in the lattice. Assuming the proposed C_y-AFM spin structure,[3,12] we use dipolar field calculation to describe these internal magnetic fields. Since the amplitude of f_4 is small and difficult to accurately estimate throughout the whole temperature range (amplitude diminishes above 50 K and there is considerable variation in the range $2 \leq T \leq 50$ K), we disregard f_4 in the calculation and aim at characterizing the other three frequencies only. The calculated internal fields ($H_{\mathrm{int},i}$, where $i=1,2,3,4$) are proportional to the ordered moment μ_{Cr} and obey $f_i = H_{\mathrm{int},i} \times 13.554$ (kHz/Oe). We find $H_{\mathrm{int},i}/\mu_{\mathrm{Cr}} = 2.5(2)$ kOe/μ_B, 3.16(7) kOe/μ_B, and 8.7(2) kOe/μ_B for $i=1-3$, respectively. We find that the ratio between the fields $H_{\mathrm{int},1}/H_{\mathrm{int},3}=0.28(9)$ and $H_{\mathrm{int},2}/H_{\mathrm{int},3}=0.36(7)$. The observed $f_1/f_3=0.367(1)$ and $f_2/f_3=0.495(2)$, thus the overall calculated result is within ~25% error. Furthermore, the absolute values of f_i allows us to estimate that the ordered moment $\mu_{\mathrm{Cr}}(1.8\ \mathrm{K}) = 1.38(22)\mu_B$. This value agrees well with the estimated $\mu_{\mathrm{ord}} = 1.2\mu_B$ from recent neutron scattering. The same calculation for a C_x-AFM structure yields that $H_{\mathrm{int},1}/H_{\mathrm{int},3} = 0.29(3)\mu_B$, $H_{\mathrm{int},2}/H_{\mathrm{int},3} = 0.88(7)\mu_B$, and $\mu_{\mathrm{Cr}}(1.8\mathrm{K}) = 1.2(4)\mu_B$. Although the C_y-AFM H_{int} ratios seem

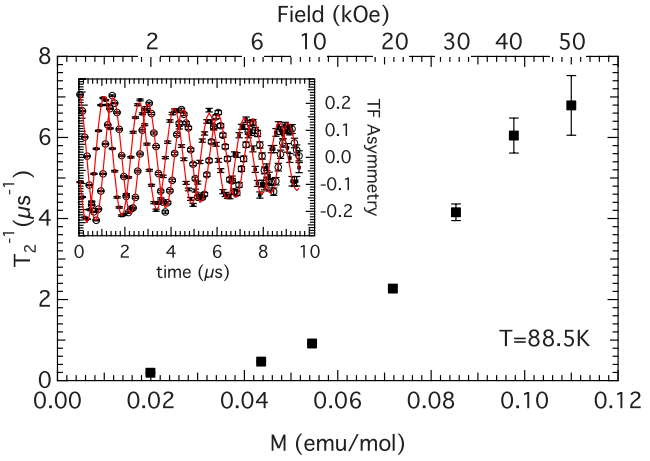

FIG. 4. (Color online) The TF relaxation rate, R_{TF} versus the magnetization, M. Inset, the muon decay asymmetry in transverse field of 2 kOe, rotated in a reference frame of 26.5 MHz.

to agree well between the calculation and the experiment, μ_{Cr} is slightly higher than the proposed C_y type but within the error. Nevertheless, it is difficult to determine which AFM structure is more reasonable for the ground state of $CaCrO_3$ based only on the present μ^+SR results. The comparison between μ_{ord} estimated by neutron and that by μ^+SR is most likely to support a C_y-AFM structure, as proposed by neutron measurements.[3]

In order to study the magnetoelastic coupling, TF μ^+SR measurements were taken at fields ranging from 2 to 50 kOe at the transition temperature. The inset of Fig. 4 plots the muon decay asymmetry in a transverse field of 2 kOe rotated at a reference frame[13] of 26.5 MHz. Since a high magnetic field is available only along the axial direction, TF measurements were performed in a spin-rotated mode, where the muon spin is rotated 90° thereby perpendicular to the field direction. The LF measurements were performed in a nonspin-rotated mode, therefore the spin and the field were parallel. No temperature dependence was found on the muon relaxation in the LF measurements, and was at least an order of magnitude smaller than the TF relaxation. It should be noted that TF measurements probe both the static and dynamic field fluctuations and the LF measurements probes the dynamic fluctuations only. Hence, it was found that the dynamic fluctuations are weak compared to the static fluctuations, therefore negligible.

The TF muon-spin polarization is best described by

$$A_0 P_{\mathrm{TF}} = A_0 \exp(-R_{\mathrm{TF}} t)\cos(\omega t + \varphi), \qquad (1)$$

where $R_{\mathrm{TF}} = (T_2^*)^{-1}$ is the TF relaxation rate and $\omega = \gamma_\mu H_{\mathrm{TF}}$. The quality of the fit is described by the solid line in the plot. Figure 4 depicts R_{TF} vs the bulk magnetization. R_{TF} increases slowly with increasing magnetization, M. At $M \sim 0.06$ emu/mol, R_{TF} increases more rapidly with M. In order to explain this occurrence, one should observe the muon behavior under external fields.

The field at the muon site is given by $\mathbf{B} = (1 + \mathbf{A}\chi)\mathbf{H}_{\mathrm{TF}}$, where $\mathbf{A}$ is the coupling between the muon and the neighboring electron. We assume that the coupling depends on the

muon-electron distance and is isotropic, therefore we write A as sum of a mean $\bar{A}$ and a fluctuating δA components. Thus one finds for a Gaussian distribution of couplings, $\rho(A) = 1/\sqrt{2\pi\sigma}\exp[-(A/\sqrt{2}\sigma)^2]$, the spectrum width obeys,[14]

$$R_{\mathrm{TF}} = \gamma_\mu M \cdot \sigma. \tag{2}$$

If $\bar{A}$ and σ are temperature independent, R_{TF} is expected to be linearly proportional to M. Figure 4 indicates that R_{TF} is not proportional or does not depend linearly on M. This suggests a modification in the hyperfine coupling, A, which is expected when lattice distortions take place.[14] In fact, by calculating the temperature dependence (for $90 \leq T \leq 130$ K, not shown) of σ, using Eq. (2), we can calculate $\Delta\sigma/\bar{\sigma}$, where $\Delta\sigma$ and $\bar{\sigma}$ are the standard deviation and average of σ, respectively. The ratio $\Delta\sigma/\bar{\sigma}$ gives a measure of the relative change in the variation in the muon-electron distance due to temperature changes. We find that $\Delta\sigma/\bar{\sigma}$ is $\sim$208%, for comparison, compounds which do not distort have a much smaller $\Delta\sigma/\bar{\sigma}$, for example, the pyrochlore $Tb_2Ti_2O_7$ has $\Delta\sigma/\bar{\sigma}$ of 15%.[15] A possible reason for such a distortion is a response of the lattice to the magnetic interactions through a magnetoelastic coupling.[16] Such coupling relieves the frustrated Cr interactions by causing lattice deformations. This is consistent with the scenario suggested by neutron-scattering studies.[3]

IV. SUMMARY

By means of μ^+SR and susceptibility, we clarified the nature of the magnetic phase of the perovskite $CaCrO_3$ below T_N. Susceptibility measurements demonstrate a presence of a weak ferromagnetic contribution in the magnetic hysteresis loops. However, μ^+SR demonstrates the formation of static AFM order below T_N. Based on electrostatic and dipole field calculations, the C_y-AFM structure, which was proposed by neutron measurements, is found to be the most reasonable in explaining the internal magnetic fields detected by zero-field μ^+SR measurements.

Transverse-field μ^+SR measurements in the paramagnetic phase provided the temperature dependence of the spin-spin relaxation rate (T_2^{-1}). The lack of a linear relationship between T_2^{-1} and magnetization above the vicinity of T_N suggests the presence of magnetoelastic coupling, which induces the abrupt change in the lattice parameters at T_N, and reduce the frustrated interactions.

Although the overall μ^+SR results confirm the past neutron results, it should be noted that the time window and spatial resolution of μ^+SR are different from those of neutron scattering. Therefore, combining the past neutron results, the magnetic and structural nature of $CaCrO_3$ have been fully elucidated by this work.

ACKNOWLEDGMENTS

We are grateful to the staff of TRIUMF for assistance with the μ^+SR experiments. J.H.B. is supported at UBC by CIfAR, NSERC of Canada, and (through TRIUMF) by NRC of Canada and K.H.C. by NSERC of Canada and (through TRIUMF) by NRC of Canada. This work is also supported by Grant-in-Aid for Scientific Research (B), Grant No. 19340107, MEXT, Japan.

*oren@triumf.ca

[1] S. V. Streltsov, M. A. Korotin, V. I. Anisimov, and D. I. Khomskii, Phys. Rev. B **78**, 054425 (2008).
[2] J.-S. Zhou, C.-Q. Jin, Y.-W. Long, L.-X. Yang, and J. B. Goodenough, Phys. Rev. Lett. **96**, 046408 (2006).
[3] A. C. Komarek, S. V. Streltsov, M. Isobe, T. Möller, M. Hoelzel, A. Senyshyn, D. Trots, M. T. Fernández-Díaz, T. Hansen, H. Gotou, T. Yagi, Y. Ueda, V. I. Anisimov, M. Grüninger, D. I. Khomskii, and M. Braden, Phys. Rev. Lett. **101**, 167204 (2008).
[4] Y. Yoshida, S. I. Ikeda, H. Matsuhata, N. Shirakawa, C. H. Lee, and S. Katano, Phys. Rev. B **72**, 054412 (2005).
[5] J. Sugiyama, Y. Ikedo, T. Goko, E. J. Ansaldo, J. H. Brewer, P. L. Russo, K. H. Chow, and H. Sakurai, Phys. Rev. B **78**, 224406 (2008).
[6] J. B. Goodenough, J. M. Longo, and J. A. Kafalas, Mater. Res. Bull. **3**, 471 (1968).
[7] J. F. Weiher, B. L. Chamberland, and J. L. Gillson, J. Solid State Chem. **3**, 529 (1971).
[8] E. Castillo-Martínez, A. Durán, and M. Á. Alario-Franco, J. Solid State Chem. **181**, 895 (2008).
[9] A. Amato and D. Andreica, *Encyclopedia of Condensed Matter Physics*, edited by Franco Bassani, Gerald L. Liedl, and Peter Wyder (Elsevier, Oxford, 2005), pp. 41–49.
[10] J. H. Brewer, *Encyclopedia of Applied Physics* (VCH, 1994), Vol. 11, pp. 23–53.
[11] G. M. Kalvius, D. R. Noakes, and O. Hartmann, *Handbook on the Physics and Chemistry of Rare Earths*, edited by K. A. Gschneidner, Jr., L Eyring, and G. H. Lander (North-Holland, Amsterdam, 2001), Vol. 32, Chap. 206.
[12] Miguel Á. Alario-Franco, E. Castillo-Martínez, and Ángel M. Arevalo-Lopez, High Press. Res. **29**, 254 (2009).
[13] T. M. Riseman and J. H. Brewer, Hyperfine Interact. **65**, 1107 (1991).
[14] P. Carretta and A. Keren, *Introduction to Frustrated Magnetism*, edited by C. Lacroix, P. Mendels, and F. Mila (Springer, Berlin, in press).
[15] O. Ofer, A. Keren, and C. Baines, J. Phys.: Condens. Matter **19**, 145270 (2007).
[16] E. Sagi, O. Ofer, A. Keren, and J. S. Gardner, Phys. Rev. Lett. **94**, 237202 (2005).